CRITICAL STUDIES ON THE KINETICS, ISOTHERMS AND ACTIVATION ENERGY OF SORPTION PHENOMENON FOR OPTIMIZED KENAF SHIVE SORBENT IN CRUDE OIL/SEAWATER SYSTEM

Abstract: The secondary effect discovery of synthetic sorbents opened another research direction for many field of studies. However, the sorption parameters of lignocellulosic sorbents are rarely reported most importantly, kenaf shive. This paper centered at the sorption behavior of optimized kenaf shive sorbents using Response Surface Methodology (RSM) via surface deposit technique. Five-level Central Composite Design (CCD) experimental matrix was used to analyze the effect of particle sizes (125-1000µm), stirring time (5-30min) and methyltrimethoxysilane (MTMS) concentration (5-20%v/v) as individual and combined variables process in the developed sorbents. The unmodified shive was compared with the modified, and it reveals a positive shift in the sorption capability. Instrumental analysis such as FTIR (Fourier Transform Infra-Red), XRD (X-ray Diffraction), DT-TGA (Differential Thermal-Thermogravimetric analysis) and BET (Brunaure-Emmett-Teller) were carried out on the optimized sorbent and the results were in conformity with the sorption results. The sorption behavior deployed fits the pseudo-first-order and Langmuir isotherm with regression coefficient R^2=0.9496 and R^2=0.9400. The sorption property was found to be spontaneous and exothermic, however, the activation energy studies shows physic-sorption phenomenon with 25.3kJmol^{-1} and R^2=0.9360.

Keywords: lignocellulosic, design matrix, sorbent, isotherm, physic-sorption.

1. Introduction

The release of organic hydrocarbon to the sea or land is termed as crude oil spillage. The broadly speaking, global energy sources are categorized into: fossil fuel, nuclear fuel, non-renewable and renewable energy resource, hitherto, crude oil is one of the common and important energy sources for transportation amongst the fossils in the planet (Ha et al., 2016; Lu et al., 2017; Zhang et al., 2017; Akhabue et al., 2018). Oil spill is majorly as result of environmental issues associated to exploration, transportation and refining (Naushad et al., 2017; Ajay et al., 2018; Bhairavi et al., 2018; Salisu et al., 2019a). Oil spills are usually transported by wind, current, temperature, weathering and salinity increases the transportation consequently, accumulate on sea surfaces or sediment at the debris (Liu et al., 2017; NOAA, 2017). This effect of oil spill is not restricted to human body directly alone, but could affect the plants within the community and water sources (Son et al., 2013; Singh et al., 2014). Furthermore, this menace affect aquatics consequently, affect the hygiene of the communities' citizenry through the inhalation of toxicants (Chang et al., 2014; ITOPF, 2014; Salisu et al., 2019b).

This menace (crude oil spill) pause a challenge upon researchers to go deep down for its containment and recovery. Containment and mechanical recovery; burning; bioremediation; chemical dispersant and the use of sorbent were approaches employed to combat this disaster (Si et al., 2015; Junaid et al., 2018; Salisu, 2019c). The concept of sorbent recovery came up in the last couple of decades. The sorbent source could be synthetic such as: polyethylene, polypropylene, polyurethane; natural inorganic such as: clay, perlite and graphite; natural organic such as: kenaf bast fibres, Sawdust and kenaf shive/core fibres (Ge et al., 2014; Mustafa et al., 2014; Shah et al., 2014; Al-Majed et al., 2015; Pickering et al., 2016; Yu et al., 2017). The sorbent technique are examples for physical methods however, biological methods using microorganisms and chemical methods using in-situ burning and dispersants are also feasible and practicable alas, the two latter are not viable (Pickering et al., 2016). The industrially acceptable physical methods for crude oil recovery is by using synthetic materials which are now considered hazardous owing to their non-biodegradability and are capital intensive (Ca et al., 2008; Wu et al., 2016; Almasian et al., 2017; Salisu et al., 2019c).

For sustainable and renewable-of course-cheap sorbents, bio-mops would need to be considered first. Kenaf plants acclimatized to different climatic changes and the bast is largely used in paper pulping, agro-packages etc. therefore, if such plant shive is modified for oil spill remediation is a long-way in research. The preeminent properties imbibe by kenaf shive are: low cost, high efficiency and biodegradable properties of natural sorbents gained a high exploration. A high number of natural organic oil sorbents were reported, namely: wood chips, sugarcane bagasse, cotton and jute (Wang, et al., 2017; Arfaoui et al., 2017). Jute plant having many a common properties with kenaf plant deems to be investigated. Jute and kenaf constitute of cellulose, hemicellulose (82-85%) and lignin (Chen et al., 2014; Na et al., 2018; Salisu et al., 2019b).

This research paper critically study the sorption behavior of this novel, ultralight, robust and facile sorbent in dense crude oil/seawater system with reference to temperature, oil concentration and sorption time.

2. EXPERIMENTAL

2.1Materials

The used chemicals are analytical grades, without further purification and dried Kenaf stalks were obtained from National Research Institute for Chemical Technology (NARICT), Zaria. The crude oil and seawater samples used for the sorption test were obtained from Petroleum Research Laboratory, Warri, Delta state, Nigeria. The raw crude oil was kept at room temperature and sea water was stored below 0^{o}Cin refrigerator.

2.2 Fabrication and hydrophobia coating of kenaf shive sorbent

The sorbents were fabricated as reported by Salisu et al., (2019c). For brevity, a pulverized Kenaf shive was dispersed in (2wt %) sodium hydroxide/urea solution (1.9wt %/10wt %) and stirred for 6mins using mechanical stirrer to achieve homogeneity in the dispersion. Aftermath, the sample was gelated by placing in a refrigerator for more than 24hrs. Then, the mixture was thawed at room temperature after frozen, followed by immersion into ethanol (99 vol %) for coagulation. The beaker in which the preparation takes place was use as mold to control the specimen thickness. It is imperative to know that no cross linker was used which makes the particles a bit loose. Coagulation was directly carried out by immersing the gel in DI water for 2 days. Freeze-drying was carried out on the sample for 2 days at approximately −60°C after pre-freezing the sample at −18°C for 12 h.

The afore-fabricated aerogel of kenaf shive was coated using chemical vapor deposition (CVD) technique for silation, i.e. methyltrimethoxysilane (MTMS). Then the resulted sample was capped and heated in an oven at 70°C for 2hrs for a completed silanation reaction. Thereafter, the coated sample was placed in a vacuum oven to remove the excess coating reagent at approximately small pressure.

2.3 Characterisations

Infrared spectra of the sorbent in KBr pellets was analysed and scanned from 4000 – 400 cm^{-1} using Shimadzu FTIR-8400S. The test was carried out on the raw (unmodified) and modified optimized unextracted sorbent that bears the highest oil sorption to confirm the modifications by taking the advantage of the unique vibration/stretching property for each functional group. The sorbent structure was determine using Shimadzu XRD 6000 (Tokyo, Japan) with CuKα radiation (λ= 1.542 Å) operated at 30 kV and 30 mA whereby the ground sorbent was scanned at rate of 0.05^{o}/min at angle range of $3^{o} \geq 2\Theta \leq 90^{o}$. The generated raw data were used to replot the diffractogram aided by **Origin Pro 9.0 16Bit**, Figure 3. Surface area was determined using Brunauer, Emmette and Teller (BET) technique by (Quantachrome Instruments, Model Nova1000e series, USA), however, the heat properties was not set aside but determine using DTA-TGA60 Shimadzu, Japan.

Comment [WU1]: No XRD presented

2.4 Adsorbability Measurement

Oil adsorption capability for both preliminaries and the optimized extacted as well as unextracted sorbent of the modified kenaf shive fibers was investigated. According to ASTM F-726-12, the adsorption capacity formula is expressed as follows (Babatope et al., 2017; Na et al., 2018; Salisu et al., 2019b):

$$S_w = \frac{S_{wt} - S_o}{S_o} \text{ ---------- (1)}$$

Where; *Sw* is the sorption rate (g (liquid)/g (sorbent)), *So* is the quality of the shive fibre before sorption, and Swt is the quality of the kenaf shive fiber after sorption. 1 g of raw and modified shive fibres was immersed into a beaker, and measurements was recorded after every 5 min. According to ASTMF-726-12, the test measures the rapid adsorption capacity (15 min soaking) and 24 h adsorption capacity. The sea water used for this test is a natural seawater not simulated.

2.5 Batch Experiments

Equal mixture of 15mL petroleum ether and 1mL of 1+1 sulfuric acid were shaken in a reparatory funnel for 15mins. The lower aqueous organic layer was released after settling for about 10min. The organic layer was poured into a beaker containing 1.2g of drying agent (anhydrous sodium sulfate), then the mixture was drain into glass funnel. Consequently, the solution was filtered into the colorimeter coupled with 25mL of petroleum ether (this was repeated with the same quantity of petroleum ether). The residual oil concentration was determined by filtering the sorbent and analysed using UV-Vis spectroscopy.

Adsorption kinetics were performed by immersing 1g of developed sorbent a mixture of oil/sea water at room temperature. Samples and crude oil concentration were, respectively, weighed and measured at different time interval, between 1-90min.

Isotherm studies was carried out at room temperature (298K) by varying the initial concentrations 5-30g/L at interval of 5g/L using the aforementioned procedure.

The adsorption thermodynamics and activation energies (Ea) were determined via the batch experiments at different temperatures (298, 303, 313 and 323K).

The crude adsorption capacity at equilibrium (Q) is calculated by the following formula:

$$Q = \frac{(C_o - C_e)V}{S} \text{ ..... (2)}$$

Where, *Co* and *Ce* are, respectively, the initial and equilibrium concentrations of crude oil (g/L) at any time t. *V* is the volume of the solution (L), and *S* is the mass of the adsorbent (g).

2.6 Adsorption kinetics

2.6.1 Pseudo first-order model

The pseudo-first-order model is represented by the following equation (Salisu et al., 2019b; Na et al., 2018):

$$\frac{dQ_t}{dt} = K_1(Q_e - Q_t) \text{..... (3)}$$

When boundary conditions are reached, $t = 0$, $Q = 0$ and $t = t$, $Q = Qt$, the equation can change to:

$$\ln(Q_e - Q_t) = lnQ_e - K_1 t \text{ ..... (4)}$$

this is simplified as:

$$Q_t = Q_e(1 - e^{-K_1 t}) \text{ ..... (5)}$$

Where, k_1 is the pseudo first-order rate constant; Qe and Qt are the adsorption capacities of the adsorbent at equilibrium.

2.6.2 Pseudo second-order model

The pseudo second-order model is represented as follows (Salisu et al., 2019b; Jingduo et al., 2015; Nwankwere et al., 2015):

$$\frac{dQt}{dt} = k_2(Q_e - Q_t)^2 \text{ ..... (6)}$$

The linearized-integrated form of the equation is:

$$Q_t = \frac{k_2 {Q_e}^2 t}{1 + k_2 Q_e t} \text{ ..... (7)}$$

where k_2 is the pseudo second-order rate constant.

2.6.3 Intraparticle diffusion model

The intraparticle diffusion model can be used to analyze the removal of pollutants by an absorbent during a diffusion process. This is expressed as the following equation (Sagnik et al., 2012; Nwankwere et al., 2015):

$$Q_t = k_p t^{0.5} + C \text{ ..... (8)}$$

where k_p is the intraparticle diffusion rate constant; and C is a constant related to the bounding layer thickness.

2.7 Adsorption Isotherm

2.7.1 Langmuir isotherm model

The Langmuir isotherm model assumes that adsorption occurs at a specific uniform location on the adsorbent surface. According to this model, the adsorbent forms a molecular monolayer.

The equation is as follows (Sagnik et al., 2012; Na et al., 2018; Salisu et al., 2019b):

$$Q_e = \frac{k_1 Q_o C_e}{1 + k_1 C_e} \text{ ..... (9)}$$

where *Qo* is the maximum adsorption capacity of the adsorbent (g/g); and K_1 is the Langmuir constant of equilibrium adsorption.

2.7.2 Freundlich isotherm model

The Freundlich isotherm model assumes that multilayer adsorption takes place at heterogeneous surfaces with different adsorption energies and characteristics. Here, the adsorption of the surface is calculated by the following equation:

$$Q_e = k_2 C_e^{\,1/n} \text{ …….. (10)}$$

where K2 (mg/g)(L/mg) 1/n is the Freundlich constant; and n is the adsorption intensity.

2.8 Adsorption Thermodynamics

The adsorption thermodynamics of the crude oil adsorption process need to be further investigated. Various thermodynamic parameters such as enthalpy (ΔH), entropy (ΔS), and Gibbs free energy (ΔG) can be obtained by isothermal adsorption studies (Boparai et al., 2011; Na, *et al.,* 2018). ΔG of adsorption can be represented by the classical Van't Hoff equation:

$$\Delta G = RT \ln Ko \text{ …….. (11)}$$

where K_0 can be calculated by the following equation:

$$K_0 = \text{Qe /Ce}$$

The apparent enthalpy (ΔH) of adsorption and the entropy (ΔS) are calculated as follows:

$$\ln\left(\frac{Q_e}{C_e}\right) = \frac{\Delta S}{T} - \frac{\Delta H}{RT} \text{ …….. (12)}$$

where ΔG is in (kJ/mol); ΔH is in (kJ/mol); ΔS is in (kJ/(molK)); R is the universal gas constant (8.314 J/mol); T is the adsorption temperature (K).

2.9 Activation energy

The activation energy can be determined from the change of the absorption rate constant, k with temperature, T(K) using the Arrhenius equation (Jingduo, *et al.,* 2015).

$$lnk = lnA - \frac{E_a}{RT} \text{ …….. (13)}$$

Where A is the pre-exponential factor obtained from the intercept plot of lnk (kinetic rate constant of the best fitted model) versus 1/T and R is the gas constant (8.314 J/mol K). By plotting ln[k] against 1/T, Ea can be calculated from the slope.

3.0 Results and Discussions

3.1. The crude oil sample was characterised using Rheometer instrument.

Table 1- Specifications of crude oil samples

Sample	**K. Viscosity (m^2/s)**	**Speed (m/s^2)**	**Torgue (Nm)**	**Temp. (^0C)**	**Density (g/cm^3)**
Crude oil	1.33	30.00	0.10	24.5	0.8965
	0.67	60.00	0.00	24.5	

In Table 1, the physical properties of the used crude oil was expatiated. Hence, viscosity and density played a vital role in adsorption. However, different crude oil have unique physical properties and were recorded, thus results the yardstick for differentiation. This is insight of the heavy crude oil. This has some difficulties in penetrating through the sorbent than the medium or light crudes (Robati, 2011; Son, *et al.*, 2013).

Table 2: Design matrix for crude oil silane (SL) modified sorbents

	Experimental Design				Results	
					Experimental	Predicted
Run no.	Resident time (min)-A	Particle size (µm)-B	MTMS conc. (%)-C	Density (gcm^{-3})	% swelling	% swelling
1	5.00	1000.00	20.00	0.075	417.10	410.7694
2	17.50	562.50	12.50	0.068	652.30	642.9804
3	17.50	1000.00	12.50	0.088	460.00	502.6942
4	17.50	562.50	20.00	0.106	778.59	881.8884
5	5.00	125.00	5.00	0.140	234.00	250.9699
6	30.50	1000.00	5.00	0.120	283.20	364.7302
7	17.50	125.00	12.50	0.058	585.60	575.1541
8	17.50	562.50	5.00	0.072	654.30	583.2501
9	5.00	562.50	12.50	0.078	181.70	353.5144
10	5.00	125.00	20.00	0.071	654.30	564.7088
11	17.50	562.50	12.50	0.102	651.60	642.9804
12	17.50	562.50	12.50	0.074	659.31	642.9804
13	30.00	125.00	5.00	0.085	290.30	322.1401
14	30.00	125.00	20.00	0.083	654.30	705.5277
15	17.50	562.50	12.50	0.079	650.57	642.9804
16	30.00	562.50	12.50	0.074	664.20	524.6339
17	17.50	562.50	12.50	0.083	654.30	642.9804
18	5.00	1000.00	5.00	0.075	222.60	163.31
19	17.50	562.50	12.50	0.083	654.30	642.9804
20	30.00	1000.00	20.00	0.073	673.30	648.2679

3.2 *Structural Characterisation*

In Figure 1 is the FTIR spectra indicating peaks of the raw (unmodified) and, modified (optimized sorbent) kenaf shive. The results are fully discussed in (Salisu et al., 2019a), for succinctness is not discussed herein. The Brunure-Emmitte-Teller (BET) result is briefly discussed here. The BET results indicates an increase in surface area from 100 to 301.1 m^2/g. This attribute to the high crude oil sorption of the optimized sorbent was observed than in the unmodified shive based on the investigated variables (see Table 2). Couple with the cementing materials effect which was vividly shown in Figure 1. The cementing material decrease the oil sorption in the sorbent because it is less porous compare to the pulverized shives (Salisu et al., 2019c).

The DT-TGA spectra in Figure 4 indicates the heat behavior and state transition of the optimized sorbent. The TG thermogram indicates four decomposition and weight loss labelled W, X, Y and Z at corresponding temperatures of 185, 355, 415 and 475^{o}C respectively. The weight loss 10% at W was as a result of dehydration and pyrolysis in the sample via endothermic heat exchange. This phenomenon was proved by DT thermogram. The second stage exothermic heat was observed resulting to weight losses at X, Y and Z corresponding to 25, 10, 50% respectively leaving 5% residue, these indicate the optimized sorbent's degradation. This attribute indicates the optimized sorbent is highly organic and decomposability consequently, eco-friendly.

Comment [WU2]: 2

Table 3: Comparative adsorption capacities of different sorbents for crude oil

Adsorbents	Maximum Sorption Capacity (g/g)	References
Crosslinked-1-Octene/styrene/DVB terpolymer	40	Yuan and Chung, 2012
Carbon fibre aerogel	115	Bi, et al.,2013
Graphene coated melamine sponge	165	Nguyen, et al., 2012
Silanized melamine sponge	163	Viet and Jame, 2014
Polypropylene	15	Jingduo et al., 2015
Banana skins	5-7	Bhraivi, et al., 2018
Silanized cellulose aerogel from paper waste	24.4	Son, et al., 2013
Acrylic acid modified kenaf shive	7	Salisu, et al.,2019a
Styrene modified kenaf shive	8.03	Salisu et al., 2019b
Silanized kenaf shive sorbent	12.02	Salisu et al., 2019c

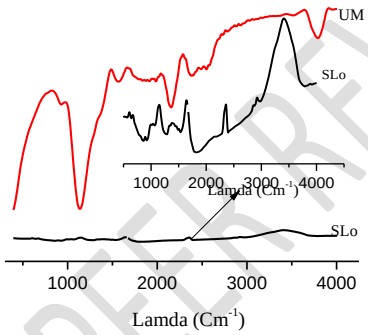

Figure 2: FTIR photogram of unmodified (UM) and optimized silane (SLo) kenaf shive sorbent

Comment [WU3]: 1

Table 4: Functional group assignment of the optimized silane kenaf shive sorbent for FTIR spectra

WAVE NUMBER (CM^{-1})	VIBRATION	STRUCTURE
786	Vs (SiC)	–Si–C
2922	δs (CH_3)	$–CH_3$
3324	δs (OH)	–OH
2051	δas(CH_2)	$–CH_2$
1673	δas(CO)	–C=O
1591	δs(CC)	$–CH=CH_2$
1151	Vs(CH_3)	$– CH_3$
1021	δs(SiOSi)	–Si–O–Si

Vs: symmetrical vibration, δs: symmetrical stretching, δas: Asymmetrical stretching

.

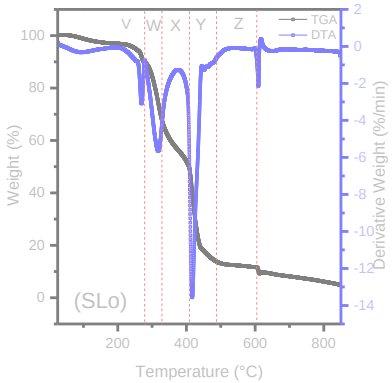

Figure 3: DT-TGA plots showing the thermal effect on the optimized modified silane sorbent

Comment [WU4]: 2

3.3 Adsorption Kinetics

Adsorption kinetics curve for the modified and optimized Kenaf Shive sorbent was exemplified in Figure 3. The relationship for the adsorption per unit time was tested in oil-water system. The slope at each point indicates the instantaneous sorption capacity. The adsorption capability increases rapidly at the initial stage i.e. 0-5min. A slow increase in adsorption was observed up to 30min, after, the curve flattens indicating equilibrium adsorption (Saha and Chowdhury, 2011; Na et al., 2018). This phenomenon was attributed to the increase in pore size of the optimized sorbent which was justified by the BET results analysis. Hence, the used oil is hydrophobic and viscose which made it slightly soluble in water, then couple with hydrophobic nature of the modifier leads to the high adsorption capability. The diffusion becomes slow when the pore sizes reduce this contributes to the slowness and little increase in sorption capacity after 30min (Salisu et al., 2019b).

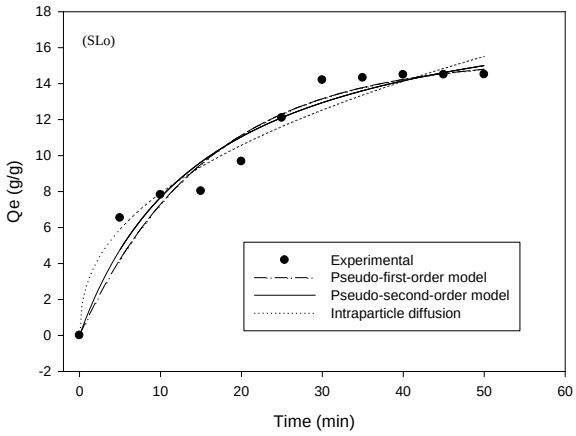

Figure 4: Kinetics of crude oil sorption on silane optimized kenaf shive sorbent

Comment [WU5]: 3

This study shows that out of the three (pseudo-first-order, pseudo-second-order and intraparticle diffusion) kinetic models used, the behavior that best fits the sorption capacity of this modified and optimized sorbent is

pseudo-first-order. This was proven by correlation coefficient (R^2) of the three said models. The R^2 of pseudo-first-order is 0.950 with sorption capacity 12.020g/g. The corresponding R^2 and sorption capacities were shown in Table 5. Despite the high adsorption shown in pseudo-second-order yet is less assured based on the recorded R^2 value (Iman et al., 2011).

Table 5: Kinetic parameters for modified/optimized kenaf shive sorption in oil/water system

Kinetic Model	Parameters	Value
Pseudo-first-order	Q_e	12.020
	K_1	0.013
	R^2	0.950
Pseudo-second-order	Q_e	15.040
	K_2	0.611
	R^2	0.843
Intraparticle diffusion	K_3	0.145
	C	8.717
	R^2	0.720

3.4 Adsorption Isotherm

Sorption isotherms describe the equilibrium existence between the liquid and solid phase, however, shows the interrelation between solute and sorbent. It is therefore, important in the sorbent optimization. Besides, it also gives the capacity of the sorbent and the equilibrium relationships between sorbent and sorbate. In other words, the ratio between the quantity sorbed and the remaining in solution at fixed temperature at equilibrium. In this study the data are fitted into prominent models; Langmuir and Freundlich isotherms. These isotherm models were depicted in Figure 4 whose constant values express the affinity of sorbate to surface of sorbent.

The Langmuir Isotherm model was developed to describe a monolayer sorption onto a solid surface of specific finite number of identical binding sites. This model shows the equilibrium distribution of sorbate onto solid or liquid sorbents with the assumption of monolayer formation on homogenous energy surface (Itodo et al., 2009). The sorption mechanisms in this model involve three steps: the diffusion of ions residue to the external surface of sorbent; the diffusion into the pores of sorbent; and the sorption of the residue on the internal surface of sorbent Nwankwere et al., (2015).

Initial concentration and contact time are the basic factors that affect the first part of this model and the final part is considered as rate determining step that is relatively quick process. Linearized form of Langmuir equation was used in this studies.

The Freundlich isotherm model is applied in the intensity estimation of sorbent towards sorbate. One major characteristic of the Freundlich isotherm, though not based on a theoretical background, is its ability to give a good representation of equilibrium data over a restricted range of concentration. The model assumes that the removal of crude oil molecules occurs on a heterogeneous sorbent surface and can be applied to multilayer sorption Nwankwere et al., (2015). The equilibrium data were treated with the linearized Freundlich isotherm equations.

The mathematical model for the adsorption isotherm for modified and optimized kenaf shive sorbent in an oil/water mixture at 313 K is presented. The results are shown in Figure 4 and Table 6. Comparison of the R^2 values (Table 5) reveals that the Langmuir model is the best fitting to explain the adsorption of crude oil from the optimized kenaf shive sorbent (SLo).

Comment [WU6]: 3

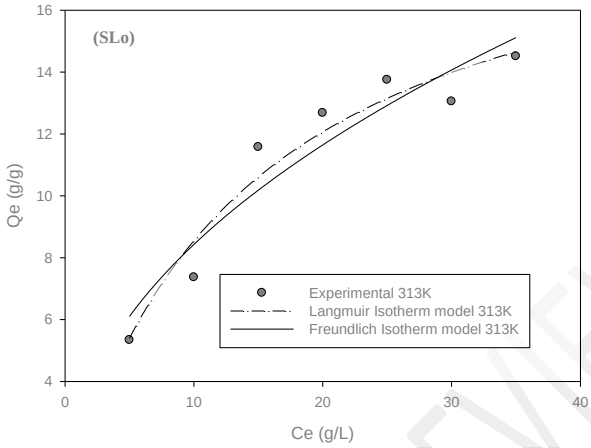

Figure 5: Isotherm of crude oil sorption on modified and optimized kenaf shive sorbent (STo)

Comment [WU7]: 4

Table 6: Thermodynamic parameters for the sorption of crude oil onto optimized kenaf shive sorbent

Isotherm Model	Isotherm Constants	Temperature (313K)
Langmuir	Q_o	12.60
	K_1	0.030
	R^2	0.940
Freundlich	n	0.600
	K_2	0.180
	R^2	0.840

3.5 Thermodynamic Studies

The thermodynamic parameters, values ΔG and ΔH can be calculated by plotting *ln(Qe/Ce)* versus *1/T* (Figure 5 and Table 7). The ΔG values of the developed sorbent ranges between approximately -1.9 to 2.8 kJ/mol at temperatures of 303, 313, 323, 333K, indicates that in the adsorption process, crude oil molecules are relatively spontaneous for the mixture on to the surface of the optimized silane sorbent. This appeared for the sorbents having a negative ΔGs, however, for positive ΔG appeared implied nonspontaneous sorption process. It also observed that as the temperature increases ΔG reduces, in other words is inversely related with temperature. Consequently, higher temperatures leads to weaker driving force of adsorption, in addition, lead to more difficult sorption of the oil (Na, *et al.*, 2018; Sajab, *et al.*, 2011). If ΔS<0, then the oil molecules movement in the developed sorbent is said to be limited and show a level of orderliness as well as decrease in randomness at the solid–mixture interface during the adsorption of crude oil/seawater system due to the highly ordered crude oil molecules in the hydrophobic layer of the sorbents at adsorption equilibrium. In other words, negative ΔS (entropy) shows an associated mechanism of the reaction and is enthalpy driven (Sagnik et al., 2012). The negative enthalpy (Δ*H*) attributed to the exothermic behavior of the sorption phenomenon (Iman et al., 2011; Salisu et al., 2019b).

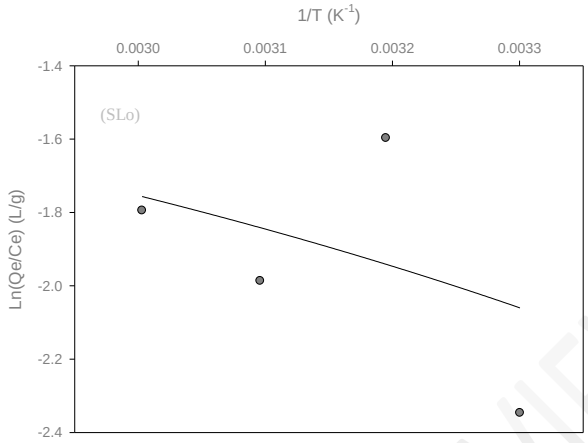

Figure 6: Plot of ln (Q_e/C_e) against $\frac{1}{T}$ for crude oil adsorption of optimized kenaf shive sorbent for thermodynamics parameters

Comment [WU8]: 5

Table 7: thermodynamics parameters for crude oil sorption on optimized kenaf shive sorbent

T (K)	ΔG (kJ.mol^{-1})	ΔH (kJ.mol^{-1})	ΔS (J.mol^{-1}.K^{-1})	Ea (kJ.mol^{-1})	R^2
303	-1.90				
313	-2.20	-7.04	-29.50	25.30	0.9360
323	-2.50				
333	-2.80				

3.6 Activation Energy

Activation energy, Ea is an important thermodynamic parameter which must be overcome by a sorbate before sorption interaction occur with the functional groups of the sorbent surface.

The activation energy can be determined from the change of the absorption rate constant, k with temperature, T (K) using the Arrhenius equation (Sajab, *et al.*, 2011):

$$lnK = lnA - \frac{E_a}{RT}$$

Where A is the pre-exponential factor and R is the gas constant (8.314 J/mol K). By plotting ln[k_1] against 1/T, E_a and lnA can be calculated respectively, from the slope and intercept. The pseudo-first-order constant was used in the activation energy manipulation because the kinetic equation that best fitted the kinetic models is the pseudo-first-order.

In this studies, the best kinetic model of each sorbent was used at different temperatures of 303, 313, 323 and 333 K. The natural logarithms of the absorption rate constants, k_1 was plotted against the 1/T. In a nut shell, the sorbents that were best fitted with say, Pseudo-first-order, the rate constant k, was determined at four different temperatures. However, such rates were plotted against the corresponding 1/T.

Plots of lnk_1 versus 1/T are presented in (Figure 6), the activation energy value is presented in Table 7.

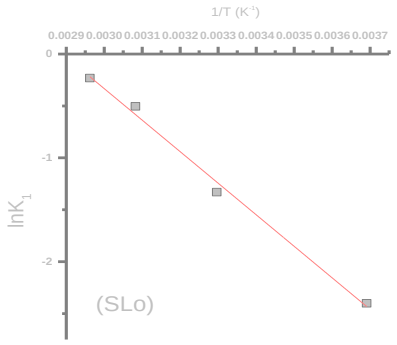

Figure 7: Plot of $\ln k_1$ against $\frac{1}{T}$ for crude oil adsorption of optimized silane kenaf shive sorbent for activation energy parameters

Comment [WU9]: 6

Generally speaking, the developed sorbent has lower activation energy because is between 5-50kJ/mol (Sajab, *et al.,* 2011; Nwankwere, *et al.,* 2015). Pseudo-second-order model has higher binding energy than those of the pseudo first-order model. This is because the corresponding models used for the absorption process controlled by chemisorption, which involves higher forces than in physic-sorption. Moreover, the physisorption phenomenon that was observed by the sorbents/mixture interface is an isosteric heat behavior of its enthalpy (ΔH) (Sidik, *et al.,* 2012).

4. Conclusion

A silanized kenaf shive sorbents were feasible via surface deposit technique. Effect of some important parameters were studied and optimized using Response Surface Methodology that increase the sorption capability to >12g/g. Containment of this menace using this agro-based waste with no/and or little economic value make an economic sense besides its eco-friendliness. To ascertain the feasibility of this facile and robust sorbent, analytical tests were carried out on the optimized sorbent such as: FTIR, BET, DT-TGA and XRD which show a backing informations to this great achievement. Of course, in order to complete the studies enthertor, a critical studies on sorption phenomenon were undertook such as: kinetics, isotherms and thermodynamics which respectively, reveals the fitness of pseudo-first-order, Langmuir and physic-sorption of the developed sorbent with an exothermic reaction process.

References

Bhairavi D.; Mika S.; Simo K. 2018. A review of bio-based materials for oil spill treatment. *Journal of Water Research* 135 (2018) 262-277

Salisu, Z.; Umaru, IS.; Danladi, A.; Yakubu, MK.; Diya'uddeen, BH. 2019a. Optimisation of crude oil adsorbent developed from a modified styrene kenaf shive. *Journal of Materials Science and Chemical Engineering, 2019, 7, 38-51, https://doi.org/10.4236/msce.2019.72004. ISSN Online: 2327-6053, ISSN Print: 2327-6045*

Liu, H., Geng, B., Chen, Y., Wang, H., 2017. Review on the aerogel-type oil sorbents derived from nanocellulose. ACS *Sutainable Chem. Eng.* 5, 49-66

NOAA, 2017b. Spill Containment Methods. Office of Response and Restoration [Online] Available at: https://response.restoration.noaa.gov/oil-and-chemicalspills/oil-spills/spill-containment-methods.html.

Chang, S.E., Stone, J., Demes, K., Piscitelli, M., 2014. Consequences of oil spills: a review and framework for informing planning. Ecol. Soc. 19 (2), 26.

ITOPF, 2014. ITOPF Response Techniques [Online] Available at: http://www.itopf. com/knowledge-resources/documents-guides/response-techniques/.

Salisu, Z.; Umaru, IS.; Danladi, A.; Yakubu, MK.; Diya'uddeen, BH. 2019b. Recovery of crude oil from aqueous medium by optimised styrene/kenaf shive graft-based sorbent via regeneration method: study of the equilibrium, kinetics and activation energy. *World Journal of Innovative Research (WJIR)*. ISSN: 2454-8236, Volume-6, Issue-2, February 2019 Pages 27-34

Singh, V.; Kendall, R. J.; Hake, K.; Ramkumar, S.; 2014 "Crude Oil Sorption by Raw Cotton" *Ind. Eng. Chem. Res.* 2013, 52, 6277.

Son, T. Nguyen; Jingduo, Feng; Nhat, T. Le Ai; T. T. Le; Nguyen, Hoang; Vincent, B. C. Tan; Hai, M. Duong; 2013, "Cellulose Aerogel from Paper Waste for Crude Oil Spill Cleaning". *Industrial and Engineering Research*, dx.doi.org/10.1021/ie4032567

Salisu, Z.M., Yakubu, M.K., Diya'uddeen B.H., Ishiaku, S.U., Abdullahi, D. 2019c. Development Of Kenaf Shive Bio–Mop Via Surface Deposit Technique For Water Remediation From Crude Oil Spill Contamination. *J. Results in Engineering*, Elsevier, dx.doi.org/10

Junaid Saleem, Muhammad Adil Riaz, Gordon McKaya. 2018. Oil sorbents from plastic wastes and polymers: A review. *Journal of Hazardous Materials* 341 (2018) 424–437. www.elsevier.com/locate/jhazmat

Si, Y., Guo, Z. 2015. Superwetting materials of oil water emulsion separation, *Chem. Lett.* 44 (2015) 874–883, http://dx.doi.org/10.1246/cl.150223.

Ge, J., Zhao, H., Zhu, H., Huang, J., Shi, L., Yu, S. 2016. Advanced sorbents for oil-spill cleanup: recent advances and future perspectives. *Advances Material* (2016)10459–10490, http://dx.doi.org/10.1002/adma.201601812.

Al-Majed, A.A., Adebayo, A.R., Hossain, M.E. 2014. A novel technology for sustainable oil spills control, *Environ. Eng. Manage. J.* 13 (2014) 265–274

Yu, L., Hao, G., Xiao,L., Yin, Q., Xia, M., Jiang,W. 2017. Robust magnetic polystyrene foam for high efficiency and removal oil from water surface, *Sep. Purif.Technol.* 173 (2017) 121–128, http://dx.doi.org/10.1016/j.seppur.2016.09.022.

Shah DU, Porter D, Vollrath F. Can silk become an effective reinforcing fibre? A property comparison with flax and glass reinforced composites. *Compos Sci Technol* 2014;101:173–83.

Mustafa A, Bin Abdollah MF, Shuhimi FF, Ismail N, Amiruddin H, Umehara N. 2015. Selection and verification of kenaf fibres as an alternative friction material using Weighted Decision Matrix method. *Mater Des* 2015;67:577–82.

Pickering, K.L., Aruan Efendy, M.G., Le, T.M. 2016. A review of recent developments in natural fibre composites and their mechanical performance. *Composites:* Part A 83 (2016) 98–112

Arfaoui, MA.; Dolez, PI.; Dube, M.; David, E. 2017. Development and characterization of hydrophobic treatment for jute fibres based on zinc oxide nanoparticles and a fatty acid. Appl. Surface Sci.397, 19-29.

Wang, A., et al., 2017. The enhanced stability and biodegradation of dispersed crude oil droplets by Xanthan Gum as an additive of chemical dispersant. *Mar. Pollut.* Bull. 118, 275-280.

Son, T. Nguyen; Jingduo, Feng; Nhat, T. Le Ai; T. T. Le; Nguyen, Hoang; Vincent, B. C. Tan; Hai, M. Duong; 2013, "Cellulose Aerogel from Paper Waste for Crude Oil Spill Cleaning". *Industrial and Engineering Research*, dx.doi.org/10.1021/4032567.

Jingduo Feng, Son T. Nguyen, Zeng Fan, Hai M. Duong. 2015. Advanced fabrication and oil absorption properties of super-hydrophobic recycled cellulose aerogels. *Chemical Engineering Journal* 270 (2015) 168–175.

Lu, Y., and Yuan, W., 2017. Superhydrophobic/Superoleophilic and Reinforced Ethyl Cellulose Sponges for Oil/Water Separation: Synergistic Strategies of Crosslinking, Carbon Nanotube Composite and Nanosilica Modification. *ACS Appl. Mater. Interfaces*, DOI: 10.1021/acsami.7b09160.

Ha HT, Son LT, Viet NTB, Dung NT, Khoi NV, et al. (2016) Oil Sorbents based on Methacrylic Acid - Grafted Polypropylene Fibers: Synthesis and Characterization. *J Chem Eng Process Technol* 7: 292. doi:10.4172/2157-7048.1000292

Sagnik Chakraborty • Shamik Chowdhury Papita Das Saha. 2012. Insight into biosorption equilibrium, kinetics and thermodynamics of crystal violet onto *Ananas comosus* (pineapple) leaf powder. *Appl Water Sci* (2012) 2:135–141, DOI 10.1007/s13201-012-0030-9

Iman Mobasherpour, Esmail Salahi, Mohsen Ebrahimi. 2011. Thermodynamics and kinetics of adsorption of Cu(II) from aqueous solutions onto multi-walled carbon nanotubes. Journal of Saudi Chemical Society 2011, 586, 302-314.

Babatope A.O., Funmilayo O. 2017. Comparative adsorption of crude oil using mango (*mangnifera indica*) shell and mango shell activated carbon. doi.org/10.4491/eer.2017.011, *University of Lagos, Lagos, Nigeria*

Zhang, C.; Chong, D.; Zhang, H.; Peng, S.; Xin, W.; Hu, Y. Regeneration of mesoporous silica aerogel for hydrocarbon adsorption and recovery. Mar. Pollut. Bull. **2017**, 122, 129–138.

Ajay, K.; Amit, K.; Gaurav, S.; Ala'a, H.; Al-M, M.N.; Ayman, A.G.; Florian, J.S. Quaternary magnetic BiOCl/g-C3N4/Cu2O/Fe3O4 nano-junction for visible light and solar powered degradation of sulfamethoxazole from aqueous environment. Chem. Eng. J. **2018**, 334, 462–478.

Naushad, M.; Ahamad, T.; Al-Maswari, B.M.; Alqadami, A.A.; Alshehri, S.M. Nickel ferrite bearing nitrogen-doped mesoporous carbon as efficient adsorbent for the removal of highly toxic metal ion from aqueous medium. Chem. Eng. J. **2017**, 330, 1351–1360.

Wu, C.J.; Li, Y.F.;Woon,W.Y.; Sheng, Y.J.; Tsao, H.K. Contact Angle Hysteresis on Graphene Surfaces and Hysteresis-free Behavior on Oil-infused Graphite Surfaces. Appl. Surf. Sci. **2016**, 385, 153–161.

Almasian, A.; Jalali, M.L.; Chizari Fard, Gh.; Maleknia, L. Surfactant grafted PDA-PAN nanofiber: Optimization of synthesis, characterization and oil absorption property. Chem. Eng. J. **2017**, 326, 1232–1241.

Wang, Z.; Ma, H.; Chu, B.; Hsiao, B.S. Super-hydrophobic modification of porous natural polymer "luffa sponge" for oil absorption. Polymer **2017**, 126, 470–476.

Ju, H.L.; Kim, D.H.; Sang, W.H.; Bo, R.K.; Park, E.J.; Jeong, M.G.; Kim, J.H.; Kim, Y.D. Fabrication of superhydrophobic fibre and its application to selective oil spill removal. Chem. Eng. J. **2016**, 289, 1–6.

Cai, S. Kimura, M. Wada, S. Kuga, L. Zhang, 2008. Cellulose aerogels from aqueous alkali hydroxide–urea solution, ChemSusChem 1 (2008) 149–154

Chen, Y.; Zhang, D., 2014. Adsorption kinetics, isotherm and thermodynamics studies of flavones from Vaccinium bracteatum Thunb leaves on NKA-2 resin, Chem. Eng. J. 254 (2014) 579–585.

Sokker, H.H., El-Sawy, N.M., Hassan, M.A., El-Anadouli, B.E. 2011. Adsorption of crude oil from aqueous solution by hydrogel of chitosan based polyacrylamide prepared by radiation induced graft polymerization, J. Hazard. Mater. 190 (2011) 359–365.

Thompson, N.E., Emmanuel, G.C., Adagadzu, K.J., Yusuf, N.B. 2010. Sorption studies of crude oil on acetylated rice husks, Arch. Appl. Sci. Res. 2 (2010) 142–151.

Boparai, H.K., Joseph, M., O'Carroll, D.M., 2011. Kinetics and thermodynamics of cadmium ion removal by adsorption onto nano zerovalent iron particles, J. Hazard. Mater. 186 (2011) 458–465.

Robati, D., 2013. Pseudo-second-order kinetic equations for modeling adsorption systems for removal of lead ions using multi-walled carbon nanotube, J. Nanostruct. Chem. 3 (2013) 55.

Saha, P., Chowdhury, S., Insight into Adsorption Thermodynamics, in: M. Tadashi (Ed.), Thermodynamics, InTech, 2011, p. 450.